ARTICLE IN PRESS

Arabian Journal of Chemistry (2016) xxx, xxx–xxx

King Saud University

Arabian Journal of Chemistry

www.ksu.edu.sa
www.sciencedirect.com

ORIGINAL ARTICLE

Effects of different mechanical treatments on structural changes of lignocellulosic waste biomass and subsequent Cu(II) removal kinetics

Zorica R. Lopičić [a,*], Mirjana D. Stojanović [a], Smilja B. Marković [b], Jelena V. Milojković [a], Marija L. Mihajlović [a], Tatjana S. Kaluđerović Radoičić [c], Mirjana L.J. Kijevčanin [c]

[a] *Institute for Technology of Nuclear and Other Mineral Raw Materials, 86 Franchet d'Esperey St., 11000 Belgrade, Serbia*
[b] *Institute of Technical Sciences of the Serbian Academy of Sciences and Arts, Knez Mihailova 35/IV, 11000 Belgrade, Serbia*
[c] *Faculty of Technology and Metallurgy, University of Belgrade, 4 Karnegijeva St., 11000 Belgrade, Serbia*

Received 29 January 2016; accepted 7 April 2016

KEYWORDS

Lignocelluloses;
Peach stone;
Mechanical treatment;
Modification;
Copper;
Biosorption kinetics

Abstract In this paper, the character of structural changes induced by different mechanical treatments to *Prunus persica* stones (PSs), and its subsequent effect on biosorption kinetics of Cu(II) were investigated. PSs were processed in vibratory disk mill (PS-V) and ultra-centrifugal mill (PS-C) and characterized by XRD, BET, SEM and FTIR spectroscopy. It was shown that PS-V was smaller and more reactive with less crystallinity index and hydrogen bond intensity compared to PS-C. In opposite, surface area of the PS-C was bigger than that of the PS-V. The total pore volume was about threefold, while the volume of micro pores was 9.29 times higher in PS-Cs than in PS-Vs.

The kinetics of Cu(II) biosorption by both PSs was tested through various kinetic models: pseudo-first and pseudo-second order rate equations, Elovich equation, Boyd model, Weber–Morris and Urano–Tachikawa intraparticle diffusion model. For both sample types, Cu(II) biosorption occurred through combination of intraparticle and film diffusion mechanism, while kinetic results were best described by the pseudo-second order kinetic model. At the same time, the results indicated that together with kinetic rate the biosorption capacity of PS-C (21.20 mg g^{-1}) was higher than that of PS-V (16.30 mg g^{-1}).

Mechanical activation like crushing and grinding will change material particle size, specific surface area and porosity, as well as its crystallinity. However, this paper elucidates that such physical

* Corresponding author at: Institute for Technology of Nuclear and Other Mineral Raw Materials, 86 Franchet d'Esperey St., 11000 Belgrade, Serbia. Tel./fax: +381 11 3691 722.
E-mail addresses: z.lopicic@itnms.ac.rs, zorica.lopicic@gmail.com (Z.R. Lopičić).

Peer review under responsibility of King Saud University.

Production and hosting by Elsevier

http://dx.doi.org/10.1016/j.arabjc.2016.04.005

Please cite this article in press as: Lopičić, Z.R. et al., Effects of different mechanical treatments on structural changes of lignocellulosic waste biomass and subsequent Cu(II) removal kinetics. Arabian Journal of Chemistry (2016), http://dx.doi.org/10.1016/j.arabjc.2016.04.005

structural changes will impact on heavy metal ions removal efficiency. This investigation suggests that the type of size reduction in lignocellulosic biosorbent preparation plays a very important role in overall biosorption performance, so it should be carefully considered every time when the mechanical treatment of material is necessary to be applied.

1. Introduction

Lignocellulosic waste (LCW) biomass represents highly valuable resource with growing worldwide role as renewable substitution for fossil fuels, alternative to expensive ion exchange resins and source of many chemicals. LCW mainly consists of cellulose, hemicellulose and lignin. These complex polymers organized in three dimensional matrixes of plant walls, are rich in functional groups, especially carboxyl and hydroxyl, which readily sequester metal ions from solutions (Torab-Mostaedi et al., 2013). However, due to its compact molecular arrangement, micro fibril structure of LCW is very rigid and tight so it is usually necessary to modify it before use. So called "opening" of this structure can be performed by single or combined physical and chemical treatments (Iddou et al., 2011; Hu et al., 2014; Gautam et al., 2014). Beside these treatments, recent intensive investigations are related to combination of two or more naturally occurring components (e.g. silica or bentonite), and some of green polymers such as lignin or chitin. This usually results in highly efficient material that combines the favorable properties of both precursors, offering many possibilities for further application (Wysokowski et al., 2014; Klapiszewski et al., 2015).

Mechanical treatment involves, at the first place, crushing and grinding necessary for particle size reduction. It represents one of the first steps in almost every sample preparation. Along with size reduction, changes in material specific surface area and porosity, as well as in its crystallinity take place (Butyagin, 1971). For this purpose, various mill types can be employed, where different forces such as friction, shear, collision, or impingement govern the modification of the LCW structure. At the same time, chemical reactivity of mechanically activated samples is enhanced because part of the mechanical energy is converted into internal energy of the substance (Boldyrev, 1986). Overall, as relatively simple and environmentally friendly, mechanical treatment can be considered as a feasible method for the pre-treatment of LCW biomass, no matter what its purpose will be (Hu et al., 2014).

In the last two decades many papers concerning LCW application as biosorbents were published. Among the other pollutants, heavy metals are the most investigated, especially because of their high toxicity, persistence and bioaccumulation tendency (Arief et al., 2008; Kumar et al., 2014). World Health Organization, has targeted chromium, cadmium, mercury, lead, copper, aluminum, cobalt, nickel, zinc, magnesium and iron as the most toxic metals, among which the copper has significant place (Djeribi and Hamdaoui, 2008). It is among the most common pollutants found in industrial effluents from electroplating, metal cleaning plating baths, mining, fertilizers, and petroleum industries (Al-Rub et al., 2006). Increased copper demand lifted by its various applications, has raised the need for copper production. In the same time, depleting ore reserves, forced the need for regeneration of the streams containing significant amounts of copper. High Cu(II) concentration in the wastewaters from the Serbian biggest mining industry, Mining and Smelting Combine Bor (RTB Bor) urged the need for alternative method which can provide reduced copper level to the 1 mg dm^{-3} (Milićević, 2015).

Biosorption, technology that uses cheap, abundant, organic waste for sequestering pollutants from wastewaters, is the most applicable when the other treatments become ineffective, particularly when the concentration of the metal ion in the solution is in the range from 10 to 100 mg l^{-1} (Cojocaru et al., 2009). Many authors have proved that peach shell has great potential for activated carbon production, but due to relatively high cost of this conversion process, it is necessary to find cheap, cost effective adsorbents, especially in developing economies such as Serbia. Peach (*Prunus persica*) has an important role in Serbia fruit production with average annual production of 96,502 t that generates approximately 17,370 t peach stone (PS) waste (Statistical office of the Republic of Serbia, 2016). PS's physical properties and chemical composition have influenced its application in most cases as a fuel (Saidur et al., 2011) or as a raw material for active carbon preparation (Uysal et al., 2014). It has also been used as mycotoxin binder (Lopičić et al., 2013a), biosorbent for dye (Marković et al., 2015) and heavy metal removal (Lopičić et al., 2013b).

Because of all of this mentioned and faced with local environment pollution problems, we have chosen to use LCW originated from PS, obtained as by-product in local fruit processing factory and investigate its possible application for Cu(II) removal.

In most papers concerning the biosorption, the effects of mechanical treatment on biomass properties are either neglected or not investigated apart from the increase of specific surface area with size reduction. Also, although some of the scientists claim that grinding process has no significant impact on overall biosorption capacity, it is confirmed that the grounded biomass more rapidly uptakes investigated metals, leading to faster equilibrium (Pavasant et al., 2006). This is very important in the design of full scale batch reactor because the data obtained from kinetic studies determine the necessary reaction time, as well as reactor dimensions (Febrianto et al., 2009).

The aim of the present study was to investigate the effects of different mechanical treatments on PSs properties and their Cu(II) biosorption performance. For the purpose of size reduction, PSs were mechanically activated by two different mill types: ultra-centrifugal mill and vibratory disk mill. Properties of the obtained particles were investigated using BET, XRD, SEM-EDX and FTIR spectroscopy. The particle size distribution was measured by laser light-scattering particle size analyzer. The biosorption kinetics was analyzed in batch experiments at different Cu(II) concentrations in order to investigate the biosorption mechanism and potential rate-controlling step. For that purpose, several kinetic models were tested: pseudo-first and pseudo-second order equation, Elovich equation, Boyd, Weber–Morris and Urano–Tachikawa model.

2. Material and methods

2.1. Biosorbent mechanical treatment

Raw PSs were randomly sampled from open landfill, near local juice and vine factory "Vino Župa", Serbia. In only two months per year, this factory generates approximately 12,000 t of biomass waste and about 2500 t relates to PSs. After sampling, PSs were separated from soft fruit residues, washed in water and dried to a constant weight at room temperature.

Grinding of PSs was performed using two mill types: vibratory disk mill "Siebtechnik – TS250" (Siebtechnik GmbH, Germany) and ultra-centrifugal mill "Retsch ZM-1" (Retsch, Gemini BV, the Netherland). In order to avoid the influence of increasing temperature during grinding, both millings were set up to 5 min. Vibratory disk mill operated discontinuously

Please cite this article in press as: Lopičić, Z.R. et al., Effects of different mechanical treatments on structural changes of lignocellulosic waste biomass and subsequent Cu(II) removal kinetics. Arabian Journal of Chemistry (2016), http://dx.doi.org/10.1016/j.arabjc.2016.04.005

in batch conditions, applying the pressure, impact and friction action, while ultra-centrifugal mill reduced particles continuously by dynamic counter-balancing of material between a rotor and a ring sieve (120 μm mesh size) applying impact and shearing on fluidized material.

After milling, particles were screened through the wire sieves with different aperture sizes. Regarding the average particle diameter d_p (mm), the samples were marked as: PS1 ($d_p < 0.1$), PS2 ($0.1 < d_p < 0.5$), PS3 ($0.5 < d_p < 1.0$), and PS4 ($1.0 < d_p < 2.0$) while the fifth fraction was whole stone with d_p approximately 3 cm, marked as PS5.

For investigation of biosorption kinetics, PSs of size less than 100 μm were used. These samples were marked as PS-V and PS-C for PSs grinded in vibratory and ultra-centrifugal mill, respectively. In order to eliminate surface impurities, the samples were washed several times in 0.001 M HCl and then in distilled water until negative reaction on Cl^- ions. The samples were dried at 60 °C to a constant weight and kept in desiccator before use.

2.2. Biosorbent characterization

The contents of crude cellulose, lignin, acid detergent fiber (ADF) and neutral detergent fiber (NDF) of PSs were determined using the ANKOM 2000 Fiber Analyzer.

The C, H, N and S contents of PS were measured in triplicate using an automatic analyzer Elementar, Vario EL III (Hanau, Germany). Oxygen content was calculated by subtraction of the ash and the C, H, N and S content from the total.

The particle size distribution was measured by the laser light-scattering particle size analyzer (PSA) (Mastersizer 2000; Malvern Instruments Ltd., Malvern, Worcestershire, U.K.). Prior to the measurement, the samples were dispersed in distilled water (22 °C), in an ultrasonic bath (at a frequency of 40 kHz and power of 50 W), for 10 min.

The surface area (SA) and the porous properties of the PS-V and PS-C biomass were determined based on N_2 adsorption–desorption isotherm at −195.8 °C on ASAP 2020 (Micromeritics Instrument Corporation, Norcross, GA, USA). Prior to the analyses, the samples were degassed at 110 °C for 10 h under reduced pressure. The SA was calculated according to the Brunauer–Emmett–Teller (BET) method from the linear part of the N_2 adsorption isotherm (Rouquerol et al., 1999). The mesopore volume (V_{meso}) and pore size distribution were analyzed according to the Barrett–Joyner–Halenda (BJH) method from the desorption isotherm (Barrett et al., 1951). The total volume of pores (V_{tot}) was given at $p/p_0 = 0.998$ while the micropore volume (V_{micro}) was evaluated by t-plot method.

Morphology of PS particles was observed using SEM model JSM – 6610LV (Jeol, Japan). Before the analyses, samples were dried 24 h at 60 °C and coated with gold.

X-ray diffraction (XRD) patterns of PS particles were obtained by step scanning, using a Philips X-ray diffractometer, model PW-1710 with Cu Kα radiation ($\lambda = 1.54178$ Å), operating at 40 kV and 30 mA while the slits for routing the primary and diffracted beams were set at 1° and 0.1 mm, respectively. The intensity of reflected rays was measured at time intervals of 0.5 s and steps of 0.02° 2θ, in the angular range from 4° to 65° 2θ. The crystalline index (CrI) was calculated according to the following equation (Kim and Holtzapple, 2006):

$$CrI = \frac{I_{002} - I_{am}}{I_{002}} \times 100\% \quad (1)$$

where I_{002} is the intensity of the cellulose crystalline peak at 22.5° 2θ, I_{am} is the peak density of amorphous cellulose, hemicellulose and lignin at 18.5° 2θ considering the shift of peaks. The estimation of comprising crystalline thickness in sample was performed by calculating the crystalline size (average crystal width) of (002) plane, D_{002}, based on Scherrer equation (Gumuskaya and Usta, 2002):

$$D_{002} = \frac{k * \lambda}{\beta \cos\theta} \quad (2)$$

where k is the Scherrer constant (0.94), λ is wavelength of X-ray tube ($\lambda = 0.154$ nm), β is full width at half maximum of (002) peak and θ represents the diffraction angle of (002) plane.

Fourier transform infrared (FTIR) spectroscopic analyses were used to determine the presence of surface functional groups in PSs. PS-V and PS-C samples were recorded using Thermo Fisher Scientific Nicolet IS-50 spectrophotometer in Attenuated Total Reflectance (ATR) mode, in the spectral range of 400–4000 cm^{-1}.

The ratio of the absorbance bands at 3345 and 1320 cm^{-1} was used to study the hydrogen bond intensity (HBI) according to the following equation (Poletto et al., 2012):

$$\mathrm{HBI} = \frac{A_{3345}}{A_{1320}} \quad (3)$$

2.3. Batch sorption experiments

Kinetic studies were performed in batch mode where 10 g l^{-1} of biosorbent (PS-V or PS-C) was placed in beakers containing different Cu(II) concentrations. The initial Cu(II) concentration ranged from 10 to 250 mg l^{-1}. Each beaker was placed on magnetic stirrer and held at constant temperature (25 °C). The stirring speed was adjusted to 250 rpm. At predetermined time intervals (5, 10, 20, 30, 45, 60, 90, 120, 180 min), aliquots of copper solutions were withdrawn, filtered immediately and sent to analysis. The analytical measurements of Cu(II) concentration in supernatants were performed using atomic absorption spectrometry (Perkin Elmer AAS Analyst 300).

The effectiveness of the process of adsorption of Cu(II) ions on the PS material was determined using the following formula (4):

$$\%\mathrm{Removal} = \frac{C_i - C_0}{C_i} \times 100\% \quad (4)$$

where C_i and C_e (mg l^{-1}) are initial and equilibrium Cu(II) ion concentration, respectively.

In all cases pH of the solutions was kept at 5, which according to our previous studies (Lopičić et al., 2013b), was established as optimal pH for Cu(II) biosorption.

Stock solution of Cu(II) (1000 mg l^{-1}) was prepared by using copper nitrate trihydrate (p.a.) salt ($Cu(NO_3)_2 \cdot 3H_2O$, Sigma–Aldrich, Germany) in deionized water. The pH adjustment was done by 0.01 M NaOH and/or 0.01 M HNO_3 solutions prepared with p.a. chemicals.

Please cite this article in press as: Lopičić, Z.R. et al., Effects of different mechanical treatments on structural changes of lignocellulosic waste biomass and subsequent Cu(II) removal kinetics. Arabian Journal of Chemistry (2016), http://dx.doi.org/10.1016/j.arabjc.2016.04.005

2.4. Biosorption kinetics

A significant part of this work was the determination of the kinetics of the process of removal Cu(II). In order to evaluate kinetic mechanism that controls the biosorption, three reaction based models are presented: Lagergren pseudo-first-order based on solid capacity, pseudo-second-order, and Elovich model. Three diffusion models were also tested to interpret the experimental data and explain the adsorption mechanism of the Cu(II) on the PSs: Boyd model, Weber–Morris and Urano–Tachikawa intraparticle diffusion model. Summarized data containing applied reaction and diffusion models are given in Table 1.

The initial sorption rate h (mg g^{-1} min^{-1}) at $t \to 0$ is calculated as follows:

$$h = k_2 q_e^2 \tag{5}$$

An approaching equilibrium factor R_E obtained from dimensionless Elovich equation (Wu et al., 2009) is defined as follows:

$$R_E = \frac{1}{q_{ref} b} \tag{6}$$

where q_{ref} is the solid phase concentration at time t_{ref} which is the longest time in adsorption process.

Linearization of Urano and Tachikawa is carried out using the initial time of contact between 0 and 180 min.

The amount of metal ions adsorbed per mass unit of adsorbent was obtained by the following equation:

$$q = \frac{(C_i - C_e) \times V}{M} \tag{7}$$

where C_i and C_e (mg l^{-1}) are initial and equilibrium Cu(II) concentration, respectively, M (g) is the mass of biosorbent and V (l) is the volume of the Cu(II) solution.

2.5. Statistical analysis and quality control

In this study, all the experiments were carried out in duplicate and the average values are presented. Adsorption of the Cu(II) on the walls of glass flasks was determined by running blank experiments, and was found to be negligible. Average values ± SD (error bars) are presented in all graphs. The correlation coefficient (R^2) values of corresponding kinetic models were determined using statistical function of Origin 9.0. The selection of the best-fit model was based on linear regression correlation coefficient (R^2), and calculated q_m values.

3. Results and discussion

3.1. Characterization of the biosorbents

3.1.1. Chemical composition

Macromolecular analysis of PS based on dry weight reveals that PS mainly consists of cellulose (62.94%), lignin (17.93%) and hemicellulose (5.42%) (Lopičić et al., 2013a, 2013b), reflecting the presence of many carboxyl and hydroxyl groups responsible for metal binding (Torab-Mostaedi et al., 2013) while the ash content was found to be 0.46%. Elemental analysis results (dry basis) show that PS contains 47.42% carbon, 6.06% hydrogen, 45,58% oxygen, 0.27% nitrogen and 0.21% sulfur.

3.1.2. Size distribution and surface area

The particle size and particle size distributions of grinded PSs for vibrational and ultra-centrifugal mill are presented in Fig. 1.

From SEM image recorded at low magnification, Fig. 1a, it can be seen that the PS-V consists of particles of non-uniform shapes and sizes. The particle size distribution is non-uniform (uniformity = 0.81), wide (*span* = 2.481) with a bimodal size distribution, Fig. 1b. The average particle size (d_{50}) for PS-V is 4.3 μm, and 10% of particles are smaller than 3.3 μm, while only 10% of particles were larger than 14 μm. Besides, PS-V is also composed of a larger fraction, with sizes between 10 and 120 μm. Fig. 1c shows that PS-C is composed of particles with similar shapes and sizes as PS-V. The particle size distribution for PS-C is non-uniform (uniformity = 0.95), wide (*span* = 3.060) and with a bimodal size distribution, Fig. 1d. The average particle size (d_{50}) is 4.5 μm, and 10% of particles are smaller than 3.3 μm, while 10% of particles are larger than 17 μm. A larger fraction was composed of particles between 10 and 100 μm.

Table 1 List of applied kinetic models.

Type	Name of kinetic model	Linear form	References
Reaction based model	Pseudo-first order	$\ln(q_e - q_t) = \ln q_e - k_1 t$	Lagergren (1898)
	Pseudo-second-order	$\frac{t}{q_t} = \frac{1}{k_2 q_e^2} + \frac{1}{q_e} t$	Ho and McKay (1999)
	Elovich	$q_t = \frac{1}{b}\ln(ab) + \frac{1}{b}\ln t$	Low (1960)
Diffusion based model	Boyd	$F = 1 - \frac{6}{\pi^2}\sum_{m=1}^{\infty}\frac{1}{m^2}\exp[-m^2 Bt]$	Boyd et al. (1947)
		$F = \frac{q_t}{q_e}$	Reichenberg (1953) for $F > 0.85$
		$B = \frac{\pi^2 D_i}{r^2}$	
		$Bt = -0.4977 - \ln(1 - F)$	
	Weber–Morris intraparticle diffusion	$q_t = k_i t^{\frac{1}{2}} + C$	Weber and Morris (1963)
	Urano–Tachikawa intraparticle diffusion	$f\left(\frac{q_t}{q_e}\right) = -\left[\log\left(1 - \left(\frac{q_t}{q_m}\right)^2\right)\right] = \frac{4\pi^2 D_i}{2.3d^2} t$	Urano and Tachikawa (1991)

k_1: pseudo-first rate constant (min^{-1}), k_2: pseudo-second-order rate constant (g mg^{-1} min^{-1}), q_t and q_e: biosorption capacities at any time t and at equilibrium, respectively (mg g^{-1}), a: initial copper biosorption rate (mg g^{-1} min^{-1}), b: extent of surface coverage and activation energy for chemisorption (g mg^{-1}), k_i: intraparticle diffusion rate constant (mg g^{-1} min$^{1/2}$), C is constant related to the thickness or boundary layer, d: particle diameter (cm), D_i: diffusion coefficient in the solid (cm^2 min^{-1}).

Please cite this article in press as: Lopičić, Z.R. et al., Effects of different mechanical treatments on structural changes of lignocellulosic waste biomass and subsequent Cu(II) removal kinetics. Arabian Journal of Chemistry (2016), http://dx.doi.org/10.1016/j.arabjc.2016.04.005

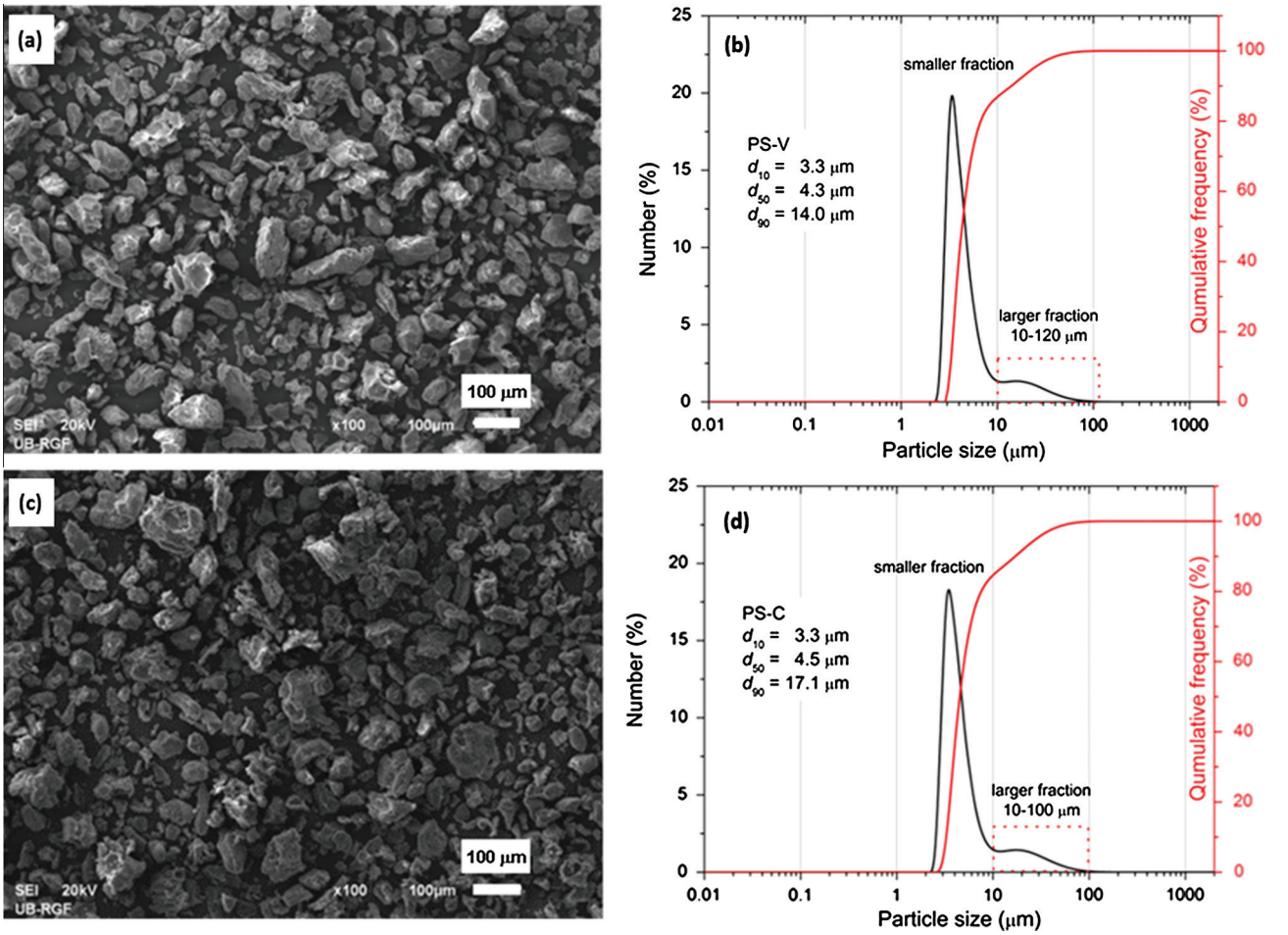

Figure 1 SEM images (a) and (c) and particle size distribution (b) and (d) of PS-V and PS-C samples.

Surface area determined by BET analyses resulted in 0.985 $m^2\ g^{-1}$ and 1.837 $m^2\ g^{-1}$, for PS-V and PS-C, respectively. The total pore volume of PS-V is 0.00288 $cm^3\ g^{-1}$ (V_{micro} = 0.000029 $cm^3\ g^{-1}$ and V_{meso} = 0.002878 $cm^3\ g^{-1}$) with the average pore diameter of 28.51 nm. For PS-C, the total pore volume was 0.00871 $cm^3\ g^{-1}$ (V_{micro} = 0.0002695 $cm^3\ g^{-1}$ and V_{meso} = 0.00835 $cm^3\ g^{-1}$) and average pore diameter was 22.21 nm. The pore sizes correspond to the mesopores, which may generally be considered as desirable for the adsorption of metal ions (Srivastava et al., 2006.).

3.1.3. XRD patterns

The XRD patterns of PS-V and PS-C are presented in Fig. 2. As can be seen, the diffraction patterns of both samples have three planes at about 15°, 17° and 22° 2θ. A sharp high peak at 2θ closed to 22.5° is assigned to the (0 0 2) plane of cellulose I. The (1 0 1) and (1 0 −1) planes of cellulose I, which are close to 14.8° and 17°, have weaker diffraction and overlap with each other. This might be due to relatively high contents of lignin and hemicellulose, which contribute to the amorphous phase of natural lignocellulose (Liao et al., 2011). It can also be seen that vibratory milling type caused the broadening of diffraction peak in (0 0 2) plane compared to ultra-centrifugal mill, which can be the result of a decrease in the percentage of crystalline phase linked with different mechanical impacts.

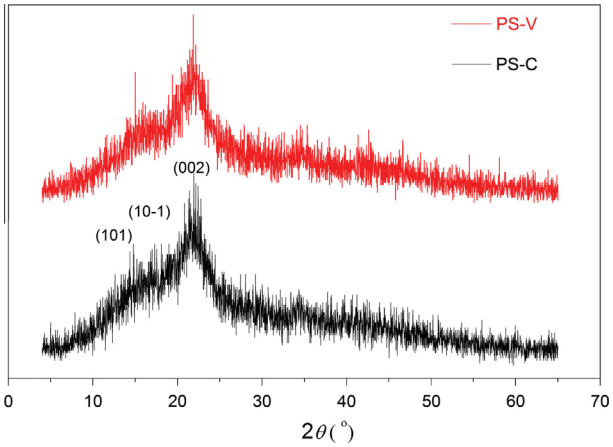

Figure 2 X-ray diffraction (XRD) patterns of PS-V and PS-C.

Both XRD patterns have the same position and location of diffraction peaks, indicating that mechanical treatment did not change the crystalline form of natural cellulose.

According to Poletto et al. (2012), the degree of cellulose crystallinity is one of the most important structure parameters because the increase in crystalline to amorphous phase ratio

Please cite this article in press as: Lopičić, Z.R. et al., Effects of different mechanical treatments on structural changes of lignocellulosic waste biomass and subsequent Cu(II) removal kinetics. Arabian Journal of Chemistry (2016), http://dx.doi.org/10.1016/j.arabjc.2016.04.005

Table 2 Physical properties of PS-V and PS-C particles.

	Average particle diameter, μm	*CrI* (%)	HBI	$D_{0\,0\,2}$ (nm)	S_{BET} ($m^2\,g^{-1}$)	V_{total} ($cm^3\,g^{-1}$)	Average pore diameter, D_{av}, nm
PS-V	4.30	35.38	0.907	2.78	0.985	0.002876	28.51
PS-C	4.50	39.16	0.982	3.66	1.837	0.008710	22.21

increases the rigidity of the sample and decreases its flexibility. The *CrI* calculated according to Eq. (1) showed that the PS-C crystallinity was higher than PS-V, 39.16–35.38%, respectively, as presented in Table 2. Obtained crystallinity indexes are similar to other natural LCW biomass that counts to 38% for native bagasse and 30% for straw (Da Silva et al., 2010). Poplar wood and wheat straw have bigger *CrI*, 50.3% and 49.9%, respectively (Barakat et al., 2013). At the same time, the apparent crystallite size ($D_{0\,0\,2}$) was higher in PS-C sample than in PS-V sample, 3.66 nm and 2.78 nm respectively. These results confirmed that PS-C sample contains more chains in highly ordered crystalline structure than PS-V sample, leading to the conclusion that vibrational milling produces sample with less degree in crystallinity and potentially higher reactivity. Similar conclusion was withdrawn by Liao et al., who obtained that 30 min ball milling of cassava stillage residue reduced the crystallinity index and crystallite size, from 44.2% to 38.4% and 2.378 nm to 2.333 nm, respectively, leading to more reactive samples (Liao et al., 2011).

The physical properties of PS-V and PS-C are summarized in Table 2.

The presented results showed that the average particle size and size distribution were similar for both samples obtained after different types of milling. On the other hand, the *CrI* is lower in PS-V than in PS-C, which was also confirmed by lower $D_{0\,0\,2}$ and HBI. Although reduction in crystallinity leads to more reactive samples, the amount of Cu(II) uptake by PS-V sample was lower than that by PS-C sample. The reason for this can be a significant reduction in surface area (of 0.985 and 1.837 $m^2\,g^{-1}$ for PS-V and PS-C, respectively) as well as the reduction of pore volume, which was about 3 times smaller in PS-V than in PS-C. Comparing the effect of surface area on Congo Red (CR) adsorption, Zhang et al. (2011) also have concluded that surface area has significant impact on dye removal. They observed that the percent removal of CR with bagasse surface area of 0.58–0.66 $m^2\,g^{-1}$ was less than 50%, while it reached 91.1% by bagasse with a surface area of 1.82 $m^2\,g^{-1}$.

3.1.4. SEM analysis

Fig. 3 shows the surface morphology of the PS-V and PS-C particles. As shown in Fig. 3a, the cross section of PS-V

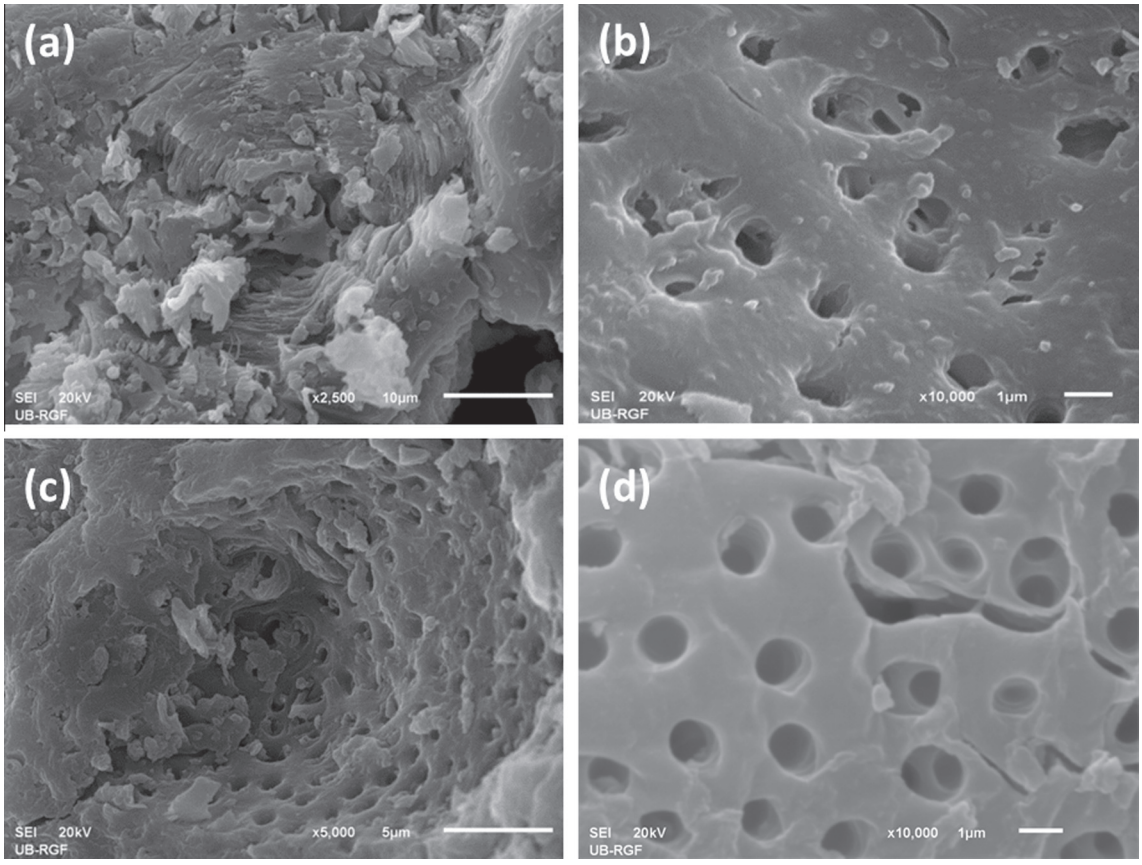

Figure 3 SEM images of cross section (a) and (c) and external layer (b) and (d) of PS-V and PS-C samples.

particle represents multilayer structure with great number of planes filled with unregularly distributed pores on the layers. The observable pore diameter is approximately 1 μm, which can be better seen in the external layers of the material (Fig. 3b). The presence of pores makes the diffusion of the solute to the internal part of the particles facilitated, which can be important for evaluating the contribution of the resistance to intraparticle diffusion on the uptake kinetics (Allouche et al., 2011). As it can be seen (Fig. 3b), the most of the external surface pores are of irregular shape, clogged with inner structural material. On the other hand, there are numerous ruptures in the layer, which might be beneficial for liquid diffusion.

The SEM micrograph of PS-C sample (Fig. 3c) also revealed the multilayer porous structure with irregular pore distribution and average pore diameter of about 1 μm (Fig. 3d). But contrary to the PS-V, the PS-C pores are more frequent and opened for diffusion into the internal parts and layers. The reason for this might be in the nature of the forces applied during milling process, which revealed more opened structure in PS-C sample resulting in better diffusion to the internal layers of the material.

3.1.5. FTIR spectroscopy

Generally, the FTIR spectra of most lignocellulosic materials can be divided into two regions: first one relates to —OH and —CH stretching vibrations (4000–2600 cm^{-1}) region, and the "fingerprint" region assigned to stretching of different functional groups present in the samples (1800–800 cm^{-1}). The most representative bands in the first region are those assigned to —OH intramolecular and intermolecular stretching modes (3600–3000 cm^{-1}) and to symmetric and asymmetric methyl and methylene groups (3000–2800 cm^{-1}) (Adel et al., 2011). A consistent strong and sharp peak typical to intramolecular hydrogen bond of cellulose I, was observed in both samples: for PS-V at 3345 cm^{-1} and for PS-C at 3346 cm^{-1}. Also, it should be noted that the peak at 1235 cm^{-1} is used to indicate the presence of structural carbohydrate such as cellulose, while the absorptions situated at 1510 and 1600 cm^{-1} (aromatic skeletal vibrations) are caused by lignin; the absorption located at 1730 cm^{-1} is caused by holocellulose-combination of cellulose and hemicellulose (*Bodirlau and Teacas, 2009*). Detailed interpretation of FTIR spectrum of PS is given by Marković et al. (2015).

It is clear from Fig. 4 that the chemical compositions of both samples are essentially the same, because the short time mechanical force did not create any new characteristic functional groups. At the same time, slight changes can be observed in the absorption peaks of the intramolecular —OH stretching vibration frequencies: the band at around 3345 cm^{-1} is more prominent for PS-C than for PS-V indicating the larger number of hydroxyl groups in PS-C, which might be connected with increasing number of inter and intramolecular hydrogen bonds formed in PS-C (Popescu et al., 2011), and higher crystallinity index. These results are in accordance with Poletto et al. (2012), which have showed that there is a positive correlation between *CrI* and amount of hydrogen bonds present in the material.

Before HBI calculation, for the sake of comparison, the FTIR spectra were normalized to 1. The calculated value of HBI for PS-C was higher compared to PS-V, 0.982 and 0.907, respectively (Table 1). This indicates that PS-C poses stronger intensity in neighboring cellulose chains, resulting in more packed structure with higher crystallinity, which was also confirmed by XRD analysis.

3.2. Biosorption kinetics

According to Djeribi and Hamdaoui (2008), four major rate steps can control the kinetics of biosorption: the first step includes mass transfer of solute from bulk solution to the

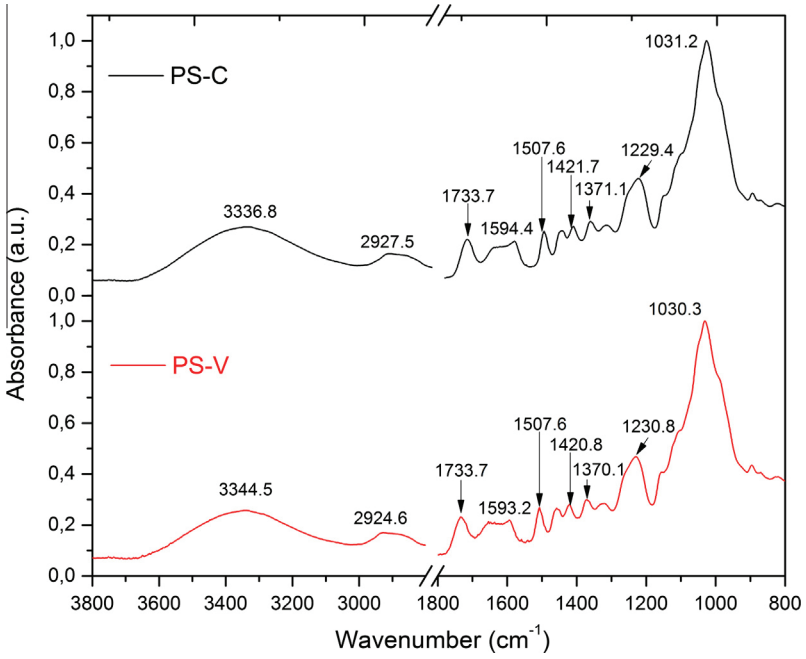

Figure 4 FTIR spectra of PS-V and PS-C.

Please cite this article in press as: Lopičić, Z.R. et al., Effects of different mechanical treatments on structural changes of lignocellulosic waste biomass and subsequent Cu(II) removal kinetics. Arabian Journal of Chemistry (2016), http://dx.doi.org/10.1016/j.arabjc.2016.04.005

boundary film and depends on agitation and solution homogeneity; the second step assumes external mass transfer by bulk diffusion of metal ions from boundary film to the biosorbent surface; the third step is internal mass transfer by diffusion of solute into the interior micro and mesopore of the biosorbent; and the last step is biosorption of ions onto the active sites through physicochemical sorption or chemical reactions such as ion exchange or complexation. It is generally accepted that the last step is quite rapid and thus cannot be the rate-determining step. Each of these steps is strongly affected by biosorbent properties.

The kinetic studies performed with PS-V samples of different sizes (Fig. 5) have showed that removal rate as well as biosorption uptake of PS-V samples increased with decrease in particle diameter. Decrease in particle size increases the equilibrium biosorption uptake from 0.55 mg g^{-1} (whole peach stone) to 3.82 mg g^{-1} (particles with diameter less than 100 μm) which, at the first place, might be attributed to the fact that smaller particles yield larger specific surface area with more active sites that are readily accessible to sorbate diffusion. It can also be seen that increase in particle size resulted in longer equilibrium time, starting from 90 to 180 min for PS1 and PS4, respectively. The initial rapid kinetics for PS1 can have significant practical importance as it could ensure process efficiency and economy at the same time, allowing the smaller reactor dimensions. So, for further experiments the fractions with diameter less than 100 μm were chosen.

The change in Cu(II) uptake with time by PS-V and PS-C at different initial Cu(II) concentrations is presented in Fig. 6. The availability of active sites on biosorbents surface caused an initial rapid metal uptake, apparent for both samples, especially for Cu(II) concentration of 10 mg l^{-1} where the equilibrium was reached in less than 10 min. For this initial concentration, amount of Cu(II) adsorbed by PS-C is lower for 13.4% than for PS-V. Increasing the driving force in the form of initial Cu(II) concentration leads to the increase in biosorption uptake for both samples, but also increased the difference between them: for initial Cu(II) concentration of 50 mg l^{-1} biosorption capacities of both samples were almost the same: 3.81 and 3.91 mg g^{-1}, while initial Cu(II) concentration of 100 mg l^{-1} resulted in capacities of 7.26 and 7.96 mg g^{-1} for PS-V and PS-C, respectively. For initial Cu (II) concentration of 250 mg l^{-1} this difference is the largest: PS-V biosorption uptake was 12.70 while the PS-C biosorption uptake was 15.48 mg g^{-1}, which is about 18% more in favor of the PS-C.

Similar trend was obtained by application of several equilibrium models, where the best fitting model was Langmuir (data not shown). This adsorption model revealed the maximum capacities of copper biosorption (q_m) 21.20 mg g^{-1} and 16.30 mg g^{-1} for PS-C and PS-V respectively. Compared with capacities of other raw biosorbents found in the literature concerning Cu(II) removal, it can be stated that mechanically treated peach stone acts like very good adsorbent. For example, dried yeast biomass has biosorption capacity 2.59 mg g^{-1} (Cojocaru et al., 2009), dried marine green macro alga *Caulerpa lentillifera* at pH = 5 has 5.57 mg g^{-1} (Pavasant et al., 2006), lentil shell has 8.98 mg g^{-1} (Aydin et al., 2008), 10.47 mg g^{-1} for spent grain (Lu and Gibb, 2008) and 25.39 mg g^{-1} for peanut shell (Witek-Krowiak et al., 2011).

The uptake vs. time profiles presented in Fig. 6 was further characterized by applying the following models to the experimental data: pseudo first- and pseudo-second-order kinetic models as well as Elovich model.

Obtained data for Lagergren pseudo-first order equation cannot be used to predict the biosorption kinetics of Cu(II) by PS. The correlation coefficient (R^2) obtained for the pseudo-first order kinetic model for the adsorption of Cu(II) ions from model solutions (concentration 10–250 mg l^{-1}) took values in the range 0.9094–0.9962 (PS-V), while for PS-C the

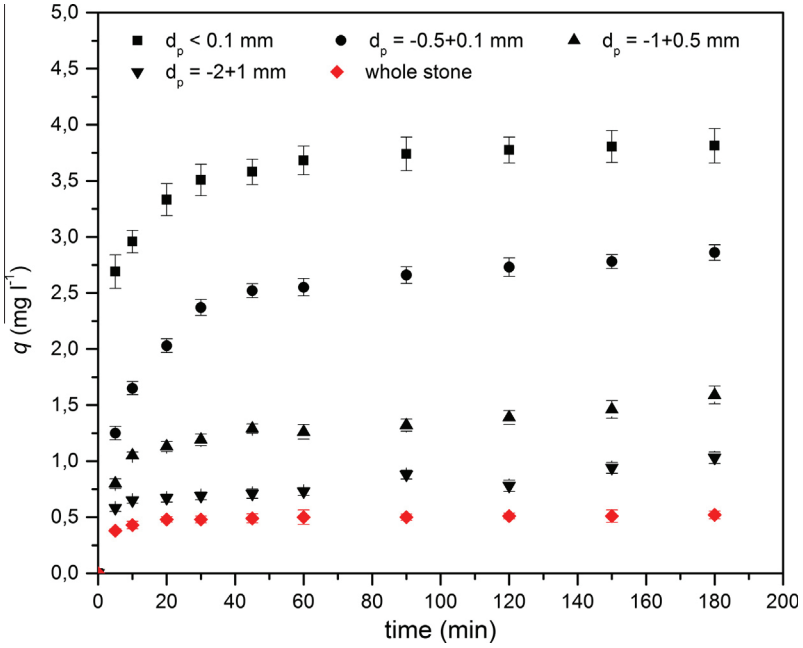

Figure 5 The amount of Cu(II) uptake of different PS-V sizes vs. time (C_i = 50 mg l^{-1}, M/V = 10 g l^{-1}, stirring speed = 250 rpm, pH = 5, T = 25 °C).

Please cite this article in press as: Lopičić, Z.R. et al., Effects of different mechanical treatments on structural changes of lignocellulosic waste biomass and subsequent Cu(II) removal kinetics. Arabian Journal of Chemistry (2016), http://dx.doi.org/10.1016/j.arabjc.2016.04.005

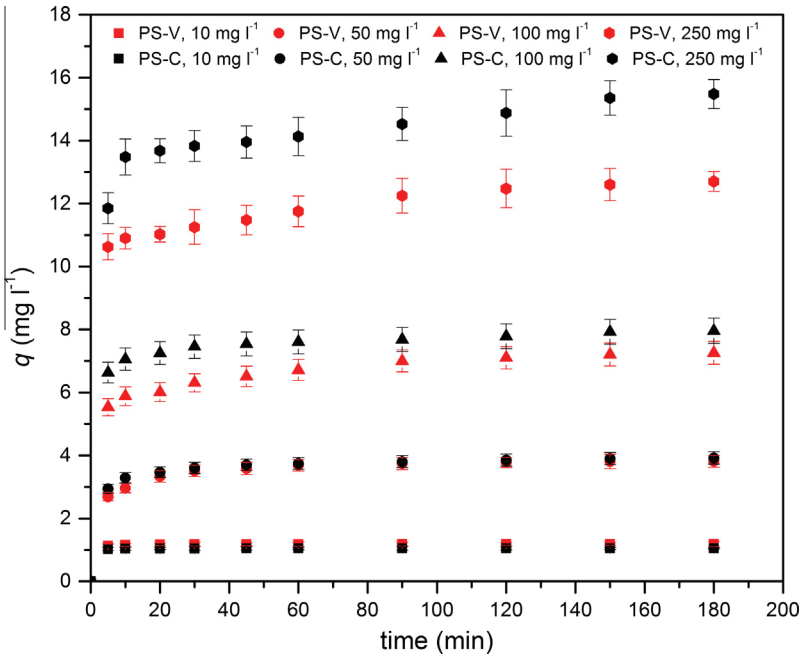

Figure 6 The amount of Cu(II) uptake by PS-V and PS-C vs. time (C_i = 10–250 mg l^{-1}, M/V = 10 g l^{-1}, stirring speed = 250 rpm, pH = 5, T = 25 °C).

R^2 range was 0.8708–0.9756. This indicates the imperfect fit of the pseudo-first-order kinetic model to the experimental data. This fact is confirmed by the discrepancies between the adsorption capacities as calculated from the pseudo-first-order kinetic model (q_m) and as determined experimentally (q_e). It was also observed that the pseudo-first order equation can be applied to kinetic data only in the initial period, where rapid biosorption of Cu(II) occurs.

Table 3 summarizes selected data for experimental biosorption uptake at equilibrium (q_e) and the values of the kinetic parameters, together with the corresponding determination coefficients (R^2).

Conversely, results presented in Table 3 show a very good compliance with the Elovich model, resulting in high correlation coefficients in the whole concentration range, meaning that kinetics of Cu(II) biosorption might also be described by chemisorption reaction. It can also be observed (Table 3) that the increase in initial Cu(II) concentration leads to the increase in constant a and to the decrease of constant b, which is in accordance with the assumption that a is a constant related to the rate of chemisorption and b is the constant related to the surface coverage. It was also noticed that both coefficients are higher for PS-C than for PS-V sample, meaning that PS-C sample has more sites available for fast biosorption of Cu(II) ions.

According to classification of characteristic curves based on R_E derived from the Elovich equation (Wu et al., 2009), there are four types of characteristic curves, depending on R_E value: if $R_E > 0.3$, then the curve rises slowly; if R_E is between 0.1 and 0.3, the curve rises mildly (mild adsorption); the value of R_E between 0.02 and 0.1 indicates rapid adsorption and when $R_E < 0.02$, the curve instantly approaches equilibrium. The values of approaching equilibrium factor, R_E, fall in the region of fast adsorption, except for initial Cu(II) concentration of 10 mg l^{-1} when an instantaneous adsorption occurred.

However, the linear form of pseudo-second-order model showed the best fit to the experimental data related to the sorption of Cu(II) on PSs with the highest squared correlation coefficients (between 0.9989 and 1.000). In addition, as shown in Table 3, the pseudo-second-order model predicted q_{m2} values were in best agreement with the experimental data. Thus, these results obtained by linear regression of experimental data, suggest that the pseudo-second order model provides the best correlation of the kinetic data. Other studies published in the literature have also reported that pseudo-second order model is applicable in the case of Cu(II) biosorption (Djeribi and Hamdaoui, 2008; Nadeem et al., 2015). Graphical presentation of kinetic modeling is given in Fig. 7.

An increase in initial Cu(II) concentration leads to the increase in equilibrium uptake capacities (q_e), initial biosorption rates (h) and the time needed for reaching the equilibrium, but it leads to the decrease of the pseudo-second order rate constant (k_2). This might indicate that the biosorption kinetics is strongly dependent on mass transfer phenomenon (Tewari et al., 2005). The initial biosorption rate of PS-V was lower than that of PS-C sample in the whole concentration range.

The biosorption performance of PS-V and PS-C particles can also be described using the proportionality index k_2q_e (min^{-1}) which is obtained by rearranging the pseudo-second order equation (Wu et al., 2009), This parameter, also known as second order rate index can be further used for calculating the half-life of the adsorption process as $t_{1/2} = 1/(k_2q_e)$ (Ofomaja and Naidoo, 2011). Calculated values of k_2q_e and $t_{1/2}$ are also displayed in Table 3. As shown in Table 3, less time is needed for PS-C than for PS-V to reduce the initial concentration by half, indicating that PS-C will approach equilibrium much faster than the PS-V.

In order to estimate which is the rate-limiting step involved in copper biosorption by PS-V and PS-C, as well as to

Please cite this article in press as: Lopičić, Z.R. et al., Effects of different mechanical treatments on structural changes of lignocellulosic waste biomass and subsequent Cu(II) removal kinetics. Arabian Journal of Chemistry (2016), http://dx.doi.org/10.1016/j.arabjc.2016.04.005

Table 3 Kinetic parameters calculated for Cu biosorption by PS-V and PS-C particles.

	Kinetic models	Initial Cu(II) concentration (mg l^{-1})			
		10	50	100	250
PS-V	Experimental q_e (mg g^{-1})	1.090	3.820	7.30	12.71
	Pseudo-second-order				
	q_m (mg g^{-1})	1.085	3.8760	7.375	12.85
	k_2 (g mg^{-1} min^{-1})	3.573	0.0838	0.0324	0.0221
	h (mg g^{-1} min^{-1})	4.213	1.259	1.746	3.655
	R^2	1.000	1.000	0.9995	1.000
	$k_2 q_e$ (min^{-1})	7.926	0.3637	0.4588	0.2727
	$t_{1/2}$ (min)	0.126	2.750	2.180	3.668
	Elovich				
	q_m (mg g^{-1})	1.096	3.935	7.268	12.57
	a (mg g^{-1} min^{-1})	7.08E + 18	4.76E + 2	5.10E + 3	2.45E + 6
	b (g mg^{-1})	41.84	3.181	1.983	1.622
	R_E	0.0222	0.0823	0.0695	0.0486
	R^2	0.9677	0.9385	0.9854	0.9321
PS-C	Experimental q_e (mg g^{-1})	0.944	3.915	7.955	15.48
	Pseudo-second-order				
	q_m (mg g^{-1})	0.9457	3.9572	7.993	15.58
	k_2 (mg g^{-1} min^{-1})	8.381	0.0919	0.0574	0.0175
	h (mg g^{-1} min^{-1})	7.496	1.439	3.670	4.254
	R^2	1.000	0.9999	0.9997	0.9989
	$k_2 q_e$ (min^{-1})	7.926	0.3637	0.4588	0.2727
	$t_{1/2}$ (min)	0.126	2.750	2.180	3.668
	Elovich				
	q_m (mg g^{-1})	0.9432	3.982	7.972	15.32
	a (mg g^{-1} min^{-1})	6.84E + 34	8.562E + 3	2.696E + 7	3.463E + 5
	b (g mg^{-1})	96.46	3.921	2.9326	1.1829
	R_E	0.010	0.0640	0.0428	0.0546
	R^2	0.9221	0.9549	0.9759	0.9177

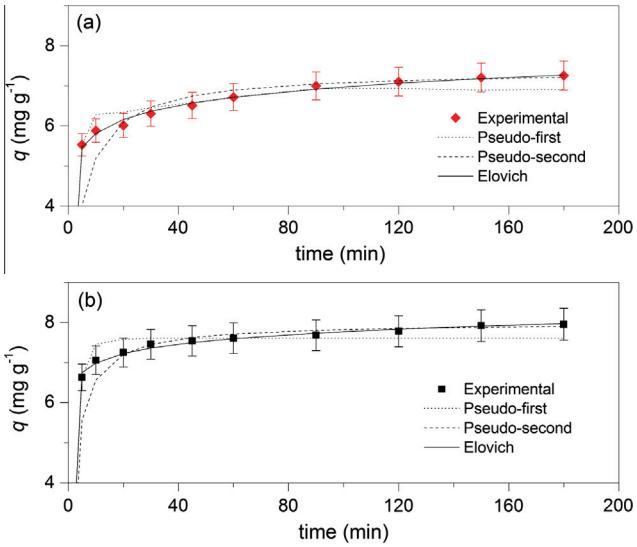

Figure 7 Regression analysis of Cu(II) uptake kinetics (a) PS-V and (b) PS-C (C_i = 100 mg l^{-1}, M/V = 10 g l^{-1}, stirring speed = 250 rpm, pH = 5, T = 25 °C).

distinguish the sorption mechanism between them, the kinetic data were further analyzed using Boyd, Weber–Morris and Urano and Tachikawa intraparticle diffusion model. The obtained results are presented in Table 4.

Using Boyd equation, the values of Bt are calculated for each fractional attainment F at time t, and plotted against time. From this plot it is possible to identify whether external transport or intraparticle diffusion controls the rate of biosorption. If the plot of Bt versus t is linear and passes through the origin, then the intraparticle diffusion is the rate limiting step. In opposite, if the fitting curve does not pass through the origin, the biosorption is governed by the external mass transport (film diffusion mechanism). It might happen that the plot of Bt versus t is multi linear: then each linear segment should be separately analyzed in order to obtain the effective diffusion coefficients from the corresponding slopes. In that case D_i is calculated as film diffusion coefficient (D_f) or pore diffusion coefficient (D_p) according to Ofomaja (2010). As shown in Fig. 8a, Boyd plot did not result in straight line passing through the origin. The multi linearity of the plot Bt vs. t meant that both diffusion processes might be responsible for mass transfer, which was also confirmed by other authors (Ofomaja and Naidoo, 2011).

For initial Cu(II) concentration of 50 mg l^{-1}, it was assumed that the film diffusion mechanism was responsible for mass transfer at first 27 min for PS-V and 25 min for PS-C, while further intraparticle diffusion takes place. The existence of transition time, which represents transition between diffusion regimes, has also been proposed by Ofomaja and Naidoo (2011).

Data from Table 4 show that the film diffusion decreased with increase of initial Cu(II) concentration, which can be explained by reduction of diffusion in the boundary layer

Table 4 Kinetic constants calculated from different diffusion models for PS-V and PS-C.

	C_i (mg l^{-1})	Weber–Morris			Boyd		Urano–Tachikawa
		k_1 (mg g^{-1} min$^{-0.5}$)	k_2 (mg g^{-1} min$^{-0.5}$)	k_3 (mg g^{-1} min$^{-0.5}$)	D_f (cm^2 min^{-1})	D_p (cm^2 min^{-1})	D_i (cm^2 min^{-1})
PS-V	10	0.0172	0.0014	0.0012	4.415E−11	1.580E−10	5.899E−11
	50	0.2887	0.1009	0.0234	1.009E−10	4.608E−10	1.345E−10
	100	0.2192	0.1744	0.0671	1.590E−11	4.190E−10	1.003E−10
	250	0.1810	0.2506	0.0915	3.563E−12	4.863E−10	1.321E−10
PS-C	10	0.0090	0.0005	0.0002	9.566E−13	3.372E−11	2.801E−11
	50	0.2288	0.0649	0.0304	5.463E−11	3.691E−10	1.174E−10
	100	0.2389	0.0729	0.0717	1.442E−11	3.733E−10	8.295E−11
	250	0.5398	0.2247	0.1069	1.041E−11	5.414E−10	1.034E−10

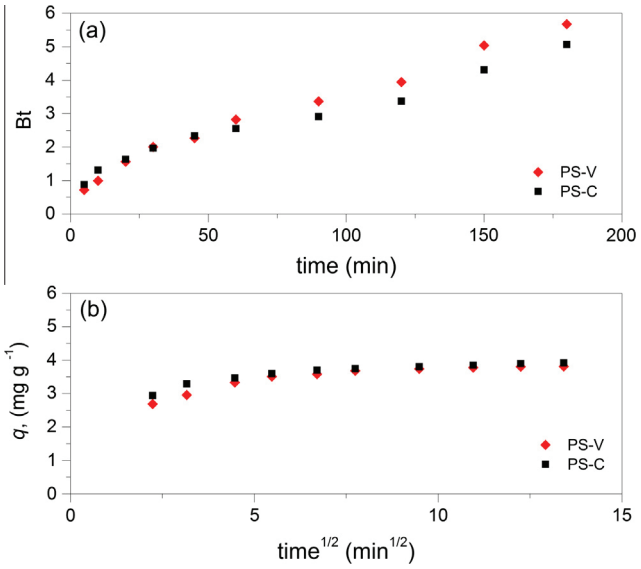

Figure 8 (a) Boyd and (b) Weber–Morris plots for the adsorption of Cu(II) onto PS-V and PS-C (C_i = 50 mg l^{-1}, M/V = 10 g l^{-1}, stirring speed = 250 rpm, pH = 5, T = 25 °C).

and the enhancement of the diffusion in the solid phase. The results also showed that $D_p > D_f$, suggesting that the film diffusion significantly controls the rate of Cu(II) diffusion. On the other hand, Singh et al. (2005) have shown that if D_p values were around 10^{-10} to 10^{-11} cm^2 s^{-1}, then intraparticle diffusion was the rate limiting step of the adsorption process. Thus, both mechanisms controlled the kinetics of biosorption process to some degree.

In theory, Weber–Morris plot between q and $t^{1/2}$ is given by several regions depending on the external mass transfer (boundary layer diffusion) followed by intraparticle diffusion in pores of different sizes; if the intraparticle diffusion is the only rate-controlling step, the plot passes through the origin, but if not, the boundary layer diffusion controls the Cu(II) removal to some degree (Cheung et al., 2007). As it can be observed from Fig. 6b, the plot of q_t versus $t^{1/2}$ does not result in a linear relationship passing through the origin, indicating that intraparticle diffusion is not the sole rate-limiting step and that biosorption is affected by more than one process. This kind of multi-linearity in the shape of the intraparticle diffusion plot has also been observed by Ofomaja (2010) in biosorption of Pb(II) onto mansonia wood sawdust. Plots for both PS-V and PS-C particles at different initial Cu(II) concentrations gave similar pattern. It could be deduced that there were three processes that controlled the rate of copper biosorption, but only one is rate limiting in particular time range. At the beginning of the process the diffusion in bulk phase to the exterior surface of the adsorbent occurs, resulting in the fastest adsorption rate. The second portion of the plot seems to refer to the diffusion into the mesopores while the third one (with the lowest slope) to the diffusion into the micropores. This implied that the intraparticle diffusion of Cu(II) ions into the micropores was the rate-limiting step in the biosorption process on PSs, especially over longer contact time and at higher concentrations. It was observed that intra-particle rate constant values k_i increased with the initial Cu(II) concentration. The correlation coefficients (R^2) for the intra-particle Weber–Morris diffusion model were between 0.9093 and 0.9856 for PS-V and between 0.9629 and 0.9856 for PS-C particles in the whole concentration range.

As it was already shown, there is a multiple nature of Cu(II) biosorption onto PSs. If the break time is defined as time when change from boundary to intraparticle diffusion occurs and this apply to the data presented in Fig. 6, it can be concluded that the change in the diffusion mechanism occurs at remarkably close times obtained from both models. According to Boyd model, at initial Cu(II) concentration of 50 mg l^{-1}, the change in diffusion mechanism occurs at 27.4 min for PS-V and 25 min for PS-C, while according to the W–M model, it occurs at 27.5 min for PS-V and 27.1 min for PS-C. Therefore, the Cu(II) biosorption by these two biosorbents occurs through combination of boundary film diffusion and intraparticle diffusion mechanism, but the overall biosorption rate is controlled by intraparticle diffusion process.

In the Urano and Tachikawa (1991) model, the adsorption rate is considered as very small and independent of the stirring speed, so the external diffusion is negligible comparing to the overall sorption rate. The diffusion coefficients D_i calculated from Urano–Tachikawa model lie in the range from 2.801E−11 to 1.345E−10 cm^2 min^{-1}. The correlation coefficients for this model indicated the poor accordance with experimental values, ranging from 0.5333 to 0.9581 for PS-C, and from 0.7977 to 0.9952 for PS-V, indicating poor accordance with experimental data.

4. Conclusion

The physical characteristics and Cu(II) biosorption aptitude of PSs obtained by vibratory disk mill (PS-V) and ultra-centrifugal mill (PS-C) were evaluated and compared. The presented results have

Please cite this article in press as: Lopičić, Z.R. et al., Effects of different mechanical treatments on structural changes of lignocellulosic waste biomass and subsequent Cu(II) removal kinetics. Arabian Journal of Chemistry (2016), http://dx.doi.org/10.1016/j.arabjc.2016.04.005

shown that the average particle size and the size distribution are similar for both types of PSs. On the other hand, the crystallinity index was lower in PS-V than in PS-C, which was also confirmed by lower crystalline thickness ($D_{0\,0\,2}$) and hydrogen bond intensity index (HBI). Although reduction in crystallinity leads to more reactive samples, the Cu(II) biosorption uptake of the PS-V was lower than that of the PS-C. The reason for this may be a significant reduction of surface area (of 0.985 and 1.837 $m^2\,g^{-1}$, for PS-V and PS-C, respectively) as well as threefold reduction of pore volume in the PS-V in relation to the PS-C. These differences are visible from the displayed SEM images, where more opened structure in PS-C sample probably resulted in better diffusion of the Cu(II) to the internal parts of the particles.

Various linear forms of kinetic models that were tested showed that in both PS-C and PS-V kinetic results were best described by the pseudo-second order kinetic model, with the following conclusions: the initial biosorption rate (h) and rate constant (k_2) were much higher for PS-C than for PS-V sample in the whole concentration range; thus, the PS-C will approach equilibrium much faster than the PS-V. This was also confirmed by Elovich equation as an existence of more sites available for fast biosorption of Cu(II) ions in PS-C than in PS-V sample. The Cu(II) biosorption by both PS-V and PS-C occurs through combination of boundary film diffusion and intraparticle diffusion mechanism with similar transition times, but the overall biosorption rate is controlled by intraparticle diffusion process. This indicates that the surface properties play a very important role in biosorption process so the grinding of dry LCW biomass must be carefully designed, because certain mechanical forces may clog the diffusion pathways and minimize overall biomass biosorption performance.

Acknowledgment

The authors are grateful to the Serbian Ministry of Education, Science and Technological Development for the financial support of this investigation included in the project TR 31003.

References

Adel, A.M., Abd El-Wahab, Z.H., Ibrahim, A.A., Al-Shemy, M.T., 2011. Characterization of microcrystalline cellulose prepared from lignocellulosic materials. Part II: Physicochemical properties. Carbohydr. Polym. 83, 676–687.

Allouche, F.N., Mameri, N., Guibal, E., 2011. Pb(II) biosorption on *Posidonia oceanica* biomass. Chem. Eng. J. 168, 1174–1184.

Al-Rub, F.A.A., El-Naas, M.H., Ashour, I., 2006. Biosorption of copper on Chlorella vulgaris from single, binary and ternary metal aqueous solutions. Process Biochem. 41, 457–464.

Arief, V.O., Trilestari, K., Sunarso, J., Indraswati, N., Ismadji, S., 2008. Recent progress on biosorption of heavy metals using low cost biosorbents: characterization, biosorption parameters and mechanism studies. CLEAN–Soil Air Water 36, 937–962.

Aydin, H., Bulut, Y., Yerlikaya, C., 2008. Removal of copper(II) from aqueous solution by adsorption onto low-cost adsorbents. J. Environ. Manage. 87, 37–45.

Barakat, A., de Vries, H., Rouau, X., 2013. Dry fractionation process as an important step in current and future lignocellulose biorefineries: a review. Bioresour. Technol. 134, 362–373.

Barrett, E.P., Joyner, L.G., Halenda, P.P., 1951. The determination of pore volume and area distribution in porous substances I. Computations from nitrogen isotherms. J. Am. Chem. Soc. 73, 373–380.

Bodirlau, R., Teacas, C.A., 2009. Fourier transform infrared spectroscopy and thermal analysis of lignocellulose fillers treated with organic anhydride. Rom. J. Phys. 54, 93–104.

Boldyrev, V.V., 1986. Mechanical activation of solids and its application to technology. J. Chim. Phys. 83, 821–829.

Boyd, G.E., Adamson, A.E., Meyers, L.S., 1947. The exchange of adsorption ions from aqueous solutions by organic zeolites II. Kinetics. J. Am. Chem. Soc. 69, 2836–2848.

Butyagin, P.Y., 1971. Kinetics and nature of mechanochemical reactions. Russ. Chem. Rev. 40, 902–915.

Cheung, W.H., Szeto, Y.S., McKay, G., 2007. Intraparticle diffusion processes during acid dye adsorption onto chitosan. Bioresour. Technol. 98 (2007), 2897–2904.

Cojocaru, C., Diaconu, M., Cretescu, I., Savić, J., Vasić, V., 2009. Biosorption of copper(II) ions from aqua solutions using dried yeast biomass. Colloids Surf. A: Physicochem. Eng. Asp. 335, 181–188.

Da Silva, A.S.A., Inoue, H., Endo, T., Yano, S., Bon, E.P.S., 2010. Milling pretreatment of sugarcane bagasse and straw for enzymatic hydrolysis and ethanol fermentation. Bioresour. Technol. 101, 7402–7409.

Djeribi, R., Hamdaoui, O., 2008. Sorption of copper(II) from aqueous solutions by cedar sawdust and crushed brick. Desalination 225, 95–112.

Febrianto, J., Kosasih, A.N., Sunarso, J., Ju, Y.H., Indraswati, N., Ismadji, S., 2009. Equilibrium and kinetic studies in adsorption of heavy metals using biosorbent: a summary of recent studies. J. Hazard. Mater. 162, 616–645.

Gautam, R.K., Mudhoo, A., Lofrano, G., Chattopadhyaya, M.C., 2014. Biomass derived biosorbents for metal ions sequestration–adsorbent modification and activation methods and adsorbent regeneration. J. Environ. Chem. Eng. 2, 239–259.

Gumuskaya, E., Usta, M., 2002. Crystalline structure properties of bleached and unbleached wheat straw (*Triticum aestivum L.*) soda–oxygen pulp. Turk. J. Agric. For. 26, 247–252.

Ho, Y.S., McKay, G., 1999. Pseudo-second order model for sorption processes. Process Biochem. 34, 451–465.

Hu, H., Zhang, Y., Liu, X., Huang, Z., Chen, Y., Yang, M., Qin, X., Feng, Z., 2014. Structural changes and enhanced accessibility of natural cellulose pretreated by mechanical activation. Polym. Bull. 71, 453–464.

Iddou, A., Hadj Youcef, M., Aziz, A., Ouali, M.S., 2011. Biosorptive removal of lead (II) ions from aqueous solutions using *Cystoseira stricta* biomass: study of the surface modification effect. J. Saudi Chem. Soc. 15, 83–88.

Kim, S., Holtzapple, M.T., 2006. Effect of structural features on enzyme digestibility of corn stover. Bioresour. Technol. 97, 583–591.

Klapiszewski, Ł., Bartczak, P., Wysokowski, M., Jankowska, M., Kabat, K., Jesionowski, T., 2015. Silica conjugated with kraft lignin and its use as a novel 'green' sorbent for hazardous metal ions removal. Chem. Eng. J. 260, 684–693.

Kumar, B., Smita, K., Flores, L.C., 2014. Plant mediated detoxification of mercury and lead. Arab. J. Chem. http://dx.doi.org/10.1016/j.arabjc.2013.08.010.

Lagergren, S., 1898. Vetenskapsakademiens. Handlingar Band 24 (4), 1–39.

Lopičić, Z., Bočarov Stančić, A., Stojanović, M., Milojković, J., Pantić, V., Adamović, M., 2013a. In vitro evaluation of the efficacy of peach stones as mycotoxin binders. Matica Srp. J. Nat. Sci. 124, 287–296.

Lopičić, Z., Milojković, J., Šoštarić, T., Petrović, M., Mihajlović, M., Lačnjevac, Č., Stojanović, M., 2013b. Influence of pH value on Cu (II) biosorption by lignocellulose peach shell waste material. Hem. Ind. 67, 1007–1015.

Liao, Z., Huang, Z., Hu, H., Zhang, Y., Tan, Y., 2011. Microscopic structure and properties changes of cassava stillage residue pretreated by mechanical activation. Bioresour. Technol. 102, 7953–7958.

Low, M.J.D., 1960. Kinetics of chemisorption of gases on solids. Chem. Rev. 60, 267–312.

Lu, S., Gibb, S.W., 2008. Copper removal from wastewater using spent-grain as biosorbent. Bioresour. Technol. 99, 1509–1517.

Marković, S., Stanković, A., Lopičić, Z., Lazarević, S., Stojanović, M., Uskoković, D., 2015. Application of raw peach shell particles for removal of methylene blue. J. Environ. Chem. Eng. 3, 716–724.

Please cite this article in press as: Lopičić, Z.R. et al., Effects of different mechanical treatments on structural changes of lignocellulosic waste biomass and subsequent Cu(II) removal kinetics. Arabian Journal of Chemistry (2016), http://dx.doi.org/10.1016/j.arabjc.2016.04.005

Milićević, Sonja, 2015. Adsorption of copper ions from mining wastewater using different mineral adsorbents (Ph.D. thesis). University of Belgrade, Serbia, Faculty of Technology and Metallurgy.

Nadeem, R., Naqvi, M.A., Nasir, M.H., Saeed, R., Iqbal, T., Ashraf, M., Ansari, T.M., 2015. Efficacy of physically pretreated *Mangifera indica* biomass for Cu^{2+} and Zn^{2+} sequestration. J. Saudi Chem. Soc. 19, 23–35.

Ofomaja, A.E., 2010. Intraparticle diffusion process for lead(II) biosorption onto mansonia wood sawdust. Bioresour. Technol. 101, 5868–5876.

Ofomaja, A.E., Naidoo, E.B., 2011. Biosorption of copper from aqueous solution by chemically activated pine cone: a kinetic study. Chem. Eng. J. 175, 260–270.

Pavasant, P., Apiratikul, R., Sungkhum, V., Suthiparinyanont, P., Wattanachira, S., Marhaba, T.H., 2006. Biosorption of Cu^{2+}, Cd^{2+}, Pb^{2+}, and Zn^{2+} using dried marine green macroalga *Caulerpa lentillifera*. Bioresour. Technol. 97, 2321–2329.

Poletto, M., Zattera, A.J., Santana, M.C.R., 2012. Structural differences between wood species: evidence from chemical composition, FTIR spectroscopy, and thermogravimetric analysis. J. Appl. Polym. Sci. 126, 336–343.

Popescu, M.-C., Lisa, G., Sakata, Y., 2011. Evaluation of morphological and chemical aspects of different wood species by spectroscopy and thermal methods. J. Mol. Struct. 988, 65–72.

Reichenberg, D., 1953. Properties of ion exchange resins in relation to their structure. III. Kinetics of exchange. J. Am. Chem. Soc. 75, 589–598.

Rouquerol, F., Rouquerol, J., Sing, K.S.W., 1999. Adsorption by Powders and Porous Solids: Principles, Methodology, and Applications. Academic Press, London.

Saidur, R., Abdelaziz, E.A., Demirbas, A., Hossain, M.S., Mekhilef, S., 2011. A review on biomass as a fuel for boilers. Renew. Sust. Energy Rev. 15, 2262–2289.

Singh, K.K., Rastogi, R., Hasan, S.H., 2005. Removal of Cr(VI) from wastewater using rice bran. J. Colloid Interface Sci. 290, 61–68.

Srivastava, V.C., Mall, I.D., Mishra, I.M., 2006. Characterization of mesoporous rice husk ash (RHA) and adsorption kinetics of metal ions from aqueous solution onto RHA. J. Hazard. Mater. 134, 257–267.

Statistical office of the Republic of Serbia, 2016. <http://webrzs.stat.gov.rs/WebSite/> (accessed 01.04.16).

Tewari, N., Vasudevan, P., Guha, B.K., 2005. Study on biosorption of Cr(VI) by *Mucor hiemalis*. Biochem. Eng. J. 23, 185–192.

Torab-Mostaedi, M., Asadollahzadeh, M., Hemmati, A., Khosravi, A., 2013. Equilibrium, kinetic, and thermodynamic studies for biosorption of cadmium and nickel on grapefruit peel. J. Taiwan Inst. Chem. Eng. 44, 295–302.

Urano, K., Tachikawa, H., 1991. Process development for removal and recovery of phosphorus from waste water by a new adsorbent 2. Adsorption rates and breakthrough curves. Ind. Eng. Chem. Res. 20, 1897–1899.

Uysal, T., Duman, G., Onal, Z., Yasa, I., Yanik, J., 2014. Production of activated carbon and fungicidal oil from peach stone by two-stage process. J. Anal. Appl. Pyrol. 108, 47–55.

Weber, W.J., Morris, J.C., 1963. Kinetics of adsorption on carbon from solution. J. Sanit. Eng. Div. Proc. Am. Soc. Civ. Eng. 89, 31–59.

Witek-Krowiak, A., Szafran, R.G., Modelski, S., 2011. Biosorption of heavy metals from aqueous solutions onto peanut shell as a low-cost biosorbent. Desalination 265, 126–134.

Wu, F.C., Tseng, R.L., Juang, R.S., 2009a. Initial behavior of intraparticle diffusion model used in the description of adsorption kinetics. Chem. Eng. J. 153, 1–8.

Wu, F.C., Tseng, R.L., Juang, R.S., 2009b. Characteristics of Elovich Equation used for the analysis of adsorption kinetics in dye-chitosan systems. Chem. Eng. J. 150, 366–373.

Wysokowski, M., Klapiszewski, Ł., Moszyński, D., Bartczak, P., Szatkowski, T., Majchrzak, I., Siwińska-Stefańska, K., Bazhenov, V.V., Jesionowski, T., 2014. Modification of chitin with kraft lignin and development of new biosorbents for removal of cadmium(ii) and nickel(ii) ions. Mar. Drugs 12, 2245–2268.

Zhang, Z., Moghaddam, L., O'Hara, I.M., Doherty, W.O.S., 2011. Congo Red adsorption by ball-milled sugarcane bagasse. Chem. Eng. J. 178, 122–128.

Please cite this article in press as: Lopičić, Z.R. et al., Effects of different mechanical treatments on structural changes of lignocellulosic waste biomass and subsequent Cu(II) removal kinetics. Arabian Journal of Chemistry (2016), http://dx.doi.org/10.1016/j.arabjc.2016.04.005